ACS OMEGA

Open Access

http://pubs.acs.org/journal/acsodf

Article

HKUST-1 Synthesis in PET Track-Etched Membranes via Conversion of Deposited Cu for Carbon Dioxide Capture

Dias D. Omertassov, Aigerim Kh. Shakayeva, Zhanna K. Zhatkanbayeva, Rafael I. Shakirzyanov, Maxim V. Zdorovets, Olgun Güven, and Ilya V. Korolkov*

Cite This: *ACS Omega* 2025, 10, 30259−30271

Read Online

ACCESS | Metrics & More | Article Recommendations | Supporting Information

ABSTRACT: Climate change remains one of the most critical global challenges, largely driven by the rise in atmospheric CO_2 levels. Effective strategies for capturing and utilizing CO_2 are crucial to mitigate its environmental impact. Metal−organic frameworks (MOFs), particularly HKUST-1 (MOF-199), are promising materials due to their high surface area, porosity, and tunable properties. In this study, HKUST-1 was successfully immobilized on polyethylene terephthalate (PET) track-etched membranes, leveraging the membranes' well-defined porosity and chemical stability. Membrane characterization via SEM revealed uniform coverage of octahedral HKUST-1 crystals with sizes ranging from 0.15 μm (inside the pores) to 1.5−5 μm (on the surface of the membrane). BET analysis of the PET TeMs-HKUST-1 composite membrane indicated a specific surface area of up to 382 m^2/g. XRD confirmed the crystallinity of the HKUST-1 structure. The composite membranes exhibited CO_2 sorption capabilities, with an adsorption capacity of 0.53 ± 0.03 mmol/g (after 1 h of adsorption) in the first cycle for the solvothermal method and 0.31 ± 0.02 mmol/g (after 1 h of adsorption) for the solvoshaker method. Durability tests demonstrated a stable performance over 12 adsorption−desorption cycles. These results highlight the potential of PET TeMs-HKUST-1 composite membranes for scalable and efficient CO_2 capture, contributing to the development of sustainable solutions for addressing climate change.

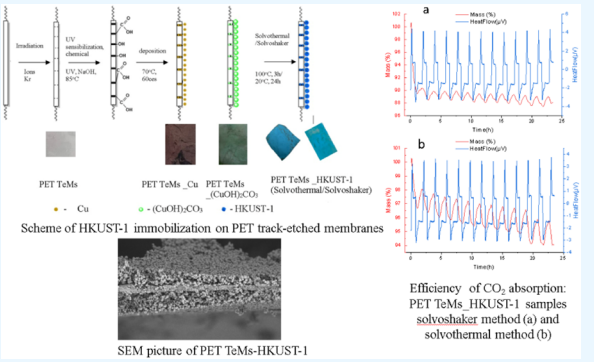

1. INTRODUCTION

Climate change is one of the major environmental challenges of our time. The increasing levels of carbon dioxide (CO_2) in the atmosphere, resulting from human activities, play a key role in intensifying the greenhouse effect and raising Earth's temperature, leading to climate changes and adverse consequences for natural ecosystems and society as a whole. Therefore, reducing CO_2 emissions has become a crucial task for ensuring stable and sustainable development.[1−3] The development of technologies to address this issue involves creating methods for capturing, storing, and using carbon dioxide. One of the most promising approaches is the use of sorption materials capable of efficiently capturing and separating CO_2 from other substances.[4−6] Among many such materials, metal−organic frameworks (MOFs) are of particular importance due to their unique properties. Metal−organic frameworks (MOFs) differ from other materials in their high adsorption capacity, attributed to their large surface area and porosity, enabling significant substance retention. Their chemical and thermal stabilities, as well as the ability to fine-tune their structure to enhance selectivity for CO_2, make MOFs versatile and highly promising for use in carbon dioxide adsorption and storage systems. These advantages make MOFs key materials in developing new technologies to mitigate the impacts of global climate change resulting from excessive release of CO_2 from anthropogenic sources.[7−11]

Metal−organic frameworks (MOFs) represent a class of crystalline porous materials composed of metal ions or clusters connected by organic ligands. This structure forms three-dimensional frameworks with highly organized pores whose size and properties can be tailored depending on the choice of components. The flexibility in selecting the geometry, size, and functionality of the components has enabled the creation of more than 20 000 different MOFs over the past decade.[12−14] The exponential growth of reticular chemistry research has led to challenges in extracting and synthesizing vast amounts of data from the literature. Zheng et al.[15] demonstrate how large language models (LLMs) can assist in streamlining this process by facilitating knowledge retrieval, synthesis optimization, and experimental automation. MOFs are formed from organic components, such as ditopic or polytopic organic carboxylates

Received: February 18, 2025
Revised: June 13, 2025
Accepted: July 7, 2025
Published: July 11, 2025

(and other negatively charged molecules), which bond with metal elements to create crystalline structures with a porosity exceeding 50% of their volume. The surface area of these MOFs typically ranges from 1000 to 10 000 m^2/g, significantly surpassing that of traditional porous materials, including zeolites and carbon-based structures. Thanks to these properties, MOFs have become one of the best options for fuel storage and applications as catalysts.[16,17] Additionally, the pores of MOFs can capture and retain various molecules, making them effective sorbents for gases and liquids, including carbon dioxide capture. By modifying the pore sizes and the functional groups on the ligands, MOFs can be tailored for selective interactions with specific molecules, which is critical for separation and catalytic processes.[18−20]

HKUST-1 is one of the most extensively studied MOF structures. This structure features a secondary building unit with a distinctive paddlewheel-like configuration, where four carboxylate groups coordinate with two Cu^{2+} ions and two solvent molecules, completing the coordination sphere. The labile solvent molecules can be removed, resulting in the formation of unsaturated metal centers. These open metal centers play a crucial role in adsorption, separation, and catalysis.[21]

Due to its porous structure, HKUST-1 possesses a significant specific surface area, making it an efficient sorbent for various molecules.[9] Additionally, HKUST-1 exhibits notable selectivity for carbon dioxide compared to other gases, such as methane or nitrogen.[22] These characteristics make HKUST-1 a promising material for applications in carbon capture and storage processes as well as in other fields requiring effective sorbents.

Track-etched membranes (TeMs) are characterized by a narrow pore size distribution, enhancing their selective properties and increasing the efficiency of separation processes. These membranes are produced from thin polymer films irradiated with heavy ions by using particle accelerators. A distinctive feature of TeMs is the regular pore structure, with the ability to adjust pore density per unit area by maintaining a narrow pore size range. This ensures high selectivity and specific operational efficiency of the membranes.[23] For instance, pore sizes can range from 50 nm to several tens of micrometers, with pore densities reaching from 10^5 to 10^{10} per square centimeter. This structure allows for the tuning of membrane transport properties for various applications, including filtration and gas separation.[24−26] TeMs are typically fabricated from polymers such as poly(ethylene terephthalate) (PET) or polycarbonate (PC), which exhibit high mechanical strength and flexibility. When MOFs are deposited onto the surface of TeMs, a composite material is formed, where the robust polymer substrate supports the fragile crystalline MOF structure, preventing its degradation under external loads. It is well-known that track-etched membranes (TeMs) are used as templates for the formation of nanostructures.[27−30] The porous structure of TeMs, composed of channels, allows for precise control over the growth and morphology of structures to be synthesized inside the pores. A study on obtaining HKUST-1 inside the pores of TeMs using an automated LBL dip-coater has demonstrated promising results for gas separation.[31] We firmly believe that further research is essential to develop improved methods for synthesizing and securely anchoring HKUST-1 on PET TeMs, with a focus on enhancing its fixation and increasing its concentration to achieve a higher adsorption capacity.

A variety of synthesis methods have been explored to produce metal−organic frameworks (MOFs), each offering unique advantages and limitations.[16] In this study, solvothermal and solvoshaker methods were employed for the immobilization of HKUST-1 on PET TeMs. The solvothermal method, which involves high-temperature and high-pressure conditions in an autoclave, is well-known for yielding highly crystalline and well-defined MOF structures.[32] However, it requires long reaction times, precise temperature control, and specialized equipment, making large-scale production challenging.[20] On the other hand, the solvoshaker method involves room-temperature synthesis with continuous agitation, allowing for lower energy consumption, reduced synthesis time, and simplified scalability.[33] Despite these advantages, solvoshaker synthesis may result in lower crystallinity and weaker MOF adhesion to the membrane compared to the solvothermal approach.[34] By comparing these two methods, this study aims to determine the most effective strategy for fabricating PET TeMs-HKUST-1 composite membranes with optimal CO_2 adsorption properties.

The aim of this study is to develop and optimize methods for synthesizing HKUST-1 on PET TeMs to create composite materials with high sorption performance for carbon dioxide (CO_2). HKUST-1 was immobilized on PET TeMs by first depositing copper microtubes in the channels, followed by their conversion into HKUST-1 using solvothermal and solvoshaker methods. These composites combine the high porosity and selectivity of MOFs with the mechanical strength and flexibility of polymer membranes, making them promising candidates for applications in gas separation and sorption systems.

2. EXPERIMENTAL PART

2.1. Preparation of TeMs. Track-etched membranes made of poly(ethylene terephthalate) (PET-TeMs) were prepared by irradiating 12 μm thick PET films (Mitsubishi Polyester Film) with $^{84}Kr^{15+}$ ions using the DC-60 accelerator with an average energy of 1.75 MeV/nucleon and an ion density of 1×10^8 ions/cm^2. The membranes were then subjected to photosensitization for 30 min on each side, followed by chemical treatment with 2.2 M NaOH at 85 °C for 180 s to produce membranes with pore sizes of approximately 300 nm.

2.2. Oxidation of PET TeMs. PET TeM samples measuring 5 × 7.5 cm were placed in a 100 mL dish, and hydrogen peroxide (37% v/v) was added to achieve the desired final concentration. The pH was maintained at 3.0 by adding a 3.0 M HCl solution.[35,36] The samples were kept in this solution for 5−10 s by occasional stirring.

2.3. Chemical Deposition of Copper on PET TeMs. The sensitization process involved immersing the samples in a solution containing 2 g of $SnCl_2$ and 2 mL of 37% HCl in 200 mL of water for 6 min, followed by thorough rinsing with hot water for 2−3 min. The samples were then activated by immersion in a solution of 0.1 g of $PdCl_2$ and 1 mL of 37% HCl in 100 mL of water for 6 min. The copper deposition was performed in a solution containing 7.63 g/L $CuSO_4 \cdot 5H_2O$, 10.26 g/L EDTA, 5 mg/L sodium lauryl sulfate, and 8.14 g/L glyoxylic acid, adjusted to a pH of 12.65−13.49 with 12.0 M KOH. The reaction was conducted at a temperature of 70 °C for 60 s.[37]

2.4. Synthesis of MOF-199 (HKUST-1) on PET TeMs. The synthesis was based on the methodology developed by the

https://doi.org/10.1021/acsomega.5c01493
ACS Omega 2025, 10, 30259−30271

authors[38] with adaptations for PET TeMs-Cu. The copper-coated PET TeMs were immersed in a 0.1 M HCl solution to remove surface oxides and then rinsed with deionized water. The cleaned samples were pretreated in a solution of 2 mL $NaHCO_3$ (1 mol/L), 2 mL $Na_2S_2O_8$ (0.05 mol/L), and 16 mL water for 24 h. Sodium persulfate ($Na_2S_2O_8$) acts as a strong oxidizing agent, introducing active functional groups (e.g., hydroxyl and carboxyl groups) on the PET surface to enhance the attachment of the MOF. Sodium bicarbonate ($NaHCO_3$) maintains a mildly alkaline environment, promoting favorable conditions for surface oxidation. Next, the PET TeMs were soaked in a solution of 0.13 g trimesic acid, 23.5 mL ethanol, and 9 mL water for 24 h. The synthesis of HKUST-1 was then carried out using trimesic acid and copper nitrate in a molar ratio of 0.5:1, with DMF, ethanol, and water in a 1:1:1 volume ratio. The process was performed in an autoclave at 80−120 °C for 3−24 h (solvothermal method). Other samples of membranes were immersed in the reaction solution and agitated using a shaker for 24 h at 20 °C (solvoshaker method). This approach allows for the formation of MOF crystals with a high degree of crystallinity and strong adhesion to the membrane surface.[39] Various synthesis parameters were investigated and are presented in Table 1.

Table 1. Parameters Used in the Synthesis of $Cu(NO_3)_2$:H_3BTC[a]

Number of recipes	Ratio $Cu(NO_3)_2$:H_3BTC	Time, h
1	0.2:0.1	3
2	0.2:0.1	6
3	0.2:0.1	24
4	0.05:0.025	3
5	0.05:0.025	6
6	0.05:0.025	24

[a]Under each condition, the reaction was carried out at 100 °C (solvothermal) and 20 °C (solvoshaker).

2.5. CO_2 Capture by PET TeMs-HKUST-1. Thermogravimetric analysis (TGA) was used to evaluate the amount of CO_2 adsorbed by the composite membranes containing HKUST-1. The adsorption test procedure consisted of three stages: degassing, adsorption, and desorption. The TeMs were placed in the sampler holder of the TGA. Degassing was performed at 150 °C for 60 min at a heating rate of 10 °C/min. The sample was then cooled to 25 °C, and the sample chamber was flushed with pure CO_2, and CO_2 adsorption was conducted for 60 min. Following this, the temperature was increased to 150 °C to perform desorption, which lasted for 60 min.

2.6. Characterization Methods. Chemical changes before and after modification of the PET TeMs were measured by a Fourier Transform Infrared (FTIR) spectrometer (InfraLUM FT-08) with an ATR accessory (GradiATR, PIKE). Spectra recordings were conducted within the range of 400−4000 cm^{-1}, utilizing 20 scans and a resolution of 2 cm^{-1} at room temperature.

The study of the surface morphology as well as the elemental composition was carried out using scanning electron microscopy (SEM) on a Phenom ProX G6 scanning electron microscope (Thermo Fisher Scientific, Eindhoven, The Netherlands) with the possibility of energy-dispersive spectroscopy.

X-ray diffraction (XRD) patterns of the samples were recorded by using a Rigaku SmartLab diffractometer under standard conditions with a Cu Kα radiation source (λ = 1.5406 Å). The diffraction patterns were recorded in Bragg−Brentano geometry (θ−θ scan) with a step size of 0.025° and a scanning speed of 3°/min.

The water contact angle (CA) was measured by using a digital microscope with 1000× magnification (Suzhou, China) at room temperature. The CA was evaluated by using the static drop method. The measurement was consecutively repeated three times at different positions. The CA was found using ImageJ 1.4.3.67 software with Drop Analysis/Drop Snake plugins.

Thermogravimetric analysis (TGA) of the samples was performed using a Themys One thermogravimetric analyzer (Setaram). The TGA was conducted in an argon atmosphere with a heating rate of 10 °C/min over a temperature range of 30−700 °C. Data analysis included recording sample mass changes (TGA) and thermal effects (HeatFlow), which were synchronously monitored. The results were used to study the thermal stability, decomposition processes, and adsorption−desorption behavior.

The surface area of the samples was measured based on N_2 adsorption isotherms using a V-Sorb 2800P BET surface area and porosity analyzer (Gold App Instruments Corp., China).

The pore size of TeMs was measured by the gas flow rate method at a pressure of 20 kPa.

3. RESULTS AND DISCUSSION

3.1. Synthesis of HKUST-1 on PET TeMs. A schematic representation of the synthesis of HKUST-1 on PET TeMs is shown in the scheme below and in Figure 1 following the experimental procedure outlined before.

Initially, the pore diameter of PET TeMs before and after copper deposition and its conversion to malachite and HKUST-1 was controlled by the gas permeability method. Thus, for the initial membranes, the pore diameter was 300 nm; after copper deposition, it decreased to 195 nm; after conversion to malachite, it was 93 nm; after the solvoshaker method (HKUST-1), it was 89 nm; and after solvothermal (HKUST-1), it was 86 nm. A decrease in gas permeability indicates a gradual filling of the pores, but nevertheless, such membranes are capable of passing gas and can be used in further applications. The slight difference between the solvoshaker and solvothermal methods indicates a thicker layer formed inside the channels for the solvothermal method.

Figure 2 shows the FTIR spectra after the process of converting copper microtubes into malachite and HKUST-1 under different conditions.

In the FTIR spectra of PET TeMs and PET TeMs-Cu and after its conversion to malachite (Figure 2a), the appearance of Cu−O absorption bands in the modified membranes indicates the formation of coordination bonds between copper ions and the functional groups of the polymer. The presence of the CO_3^{2-} absorption band in the spectrum of the membrane after conversion to malachite confirms the presence of this compound in the composite.

Figure 2b,c presents the FTIR spectra of four HKUST-1 samples synthesized using different methods and processing durations and also the spectrum of commercial HKUST-1 for comparison. All spectra exhibit characteristic bands indicative of the presence of a metal−organic framework structure. In the 500−700 cm^{-1} region, bands corresponding to Cu−O

https://doi.org/10.1021/acsomega.5c01493
ACS Omega 2025, 10, 30259−30271

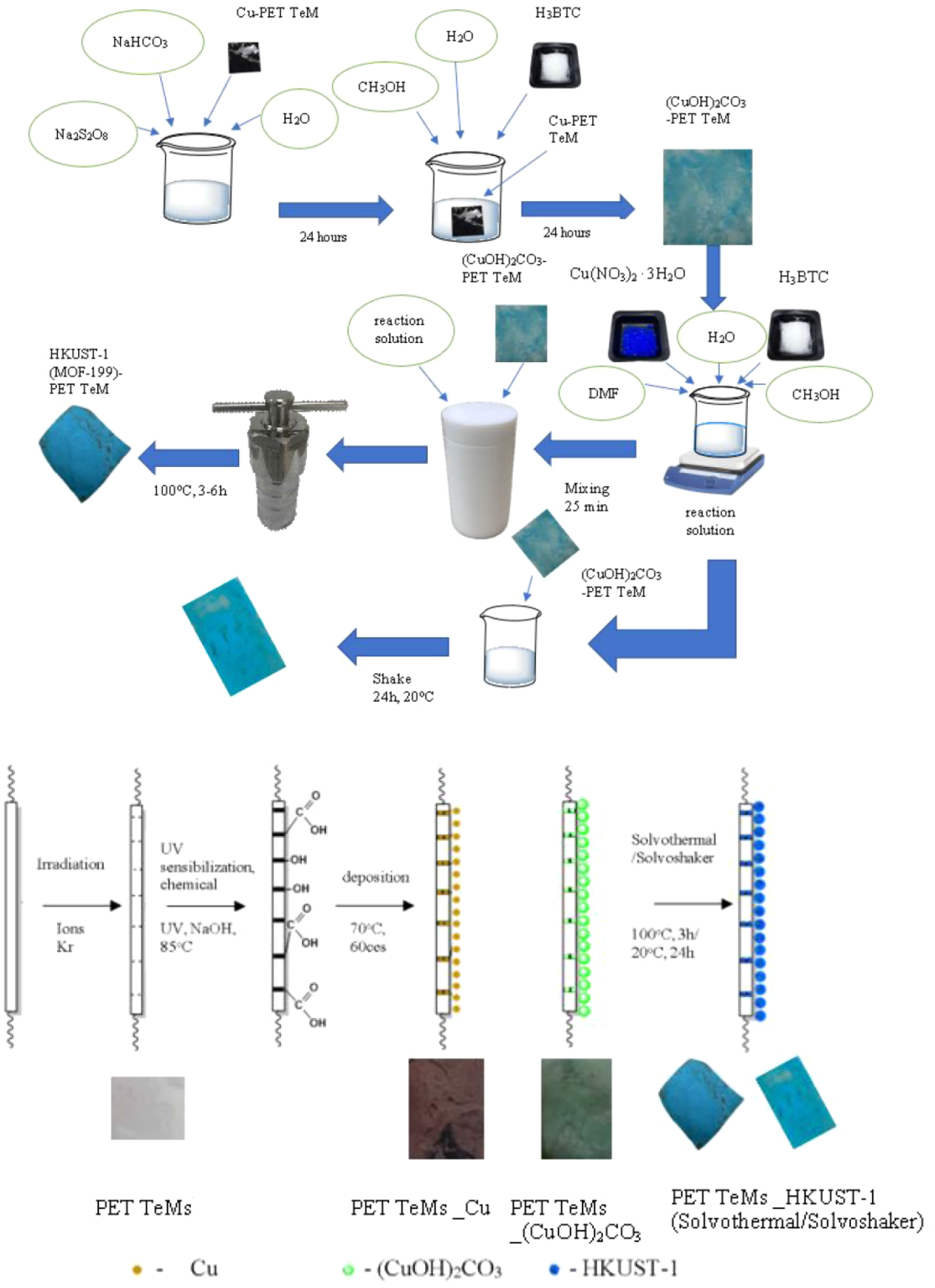

Figure 1. Scheme of synthesis of HKUST-1 by solvothermal/solvoshaker methods*. **Photograph of samples courtesy of Dias D. Omertassov. Copyright 2025.*

vibrations are observed, confirming the presence of metallic centers within the framework. The 1400−1600 cm^{-1} range is characterized by bands associated with vibrations of COO^- groups interacting with copper, indicating the successful formation of coordination bonds with trimesic acid. These bands are present in all samples, but their intensity varies, depending on the synthesis method and processing time. The FTIR spectra obtained in our study were analyzed and compared to previously published data for HKUST-1 (MOF-199). The presence of strong stretching vibrations of carboxylate groups around 1400−1600 cm^{-1}, as observed in our spectra, is consistent with the characteristic $-COO^-$ vibrations reported in the literature,[40,41] confirming the coordination between copper ions and the carboxylic groups

https://doi.org/10.1021/acsomega.5c01493
ACS Omega 2025, 10, 30259−30271

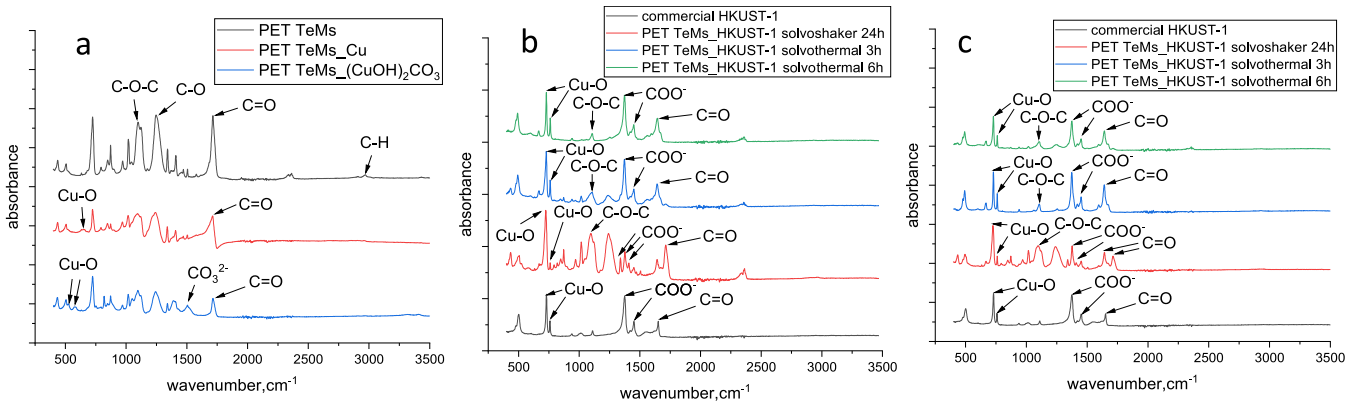

Figure 2. FTIR of PET TeMs, PET TeMs-Cu, and after conversion to malachite (a), and after synthesis of HKUST-1 under different conditions, obtained at a ratio of $Cu(NO_3)_2$:H_3BTC = 0.2:0.1 g (b) and 0.05:0.025 g (c).

of trimesic acid. It is also clearly seen that when using the solvothermal method, compared with solvoshaking, the peaks related to the PET TeMs (such as the bands around ∼1710 cm^{-1} and ∼1100−1250 cm^{-1}) become less intense, while the peaks related to HKUST-1 (Cu−O and COO^- groups) exhibit higher intensity. This observation suggests that the PET substrate is more extensively covered by the HKUST-1 phase when the solvothermal method is applied, resulting in attenuation of the polymer's characteristic signals and enhancement of MOF-related features. These spectral differences indicate the formation of a thicker and more uniform HKUST-1 layer on the membrane surface under solvothermal conditions, which aligns with expectations based on synthesis duration and conditions. The difference in the thickness of the deposited layer is also confirmed by SEM.

The SEM cross-section images in Figure 3 of the PET membrane−HKUST-1 obtained by solvothermal and solvoshaker methods show the presence of a layered substrate structure. On the membrane surface, octahedral crystals corresponding to the HKUST-1 structure are visible, attached to the substrate with the average crystal size being 2.6 μm for the solvothermal method. The octahedral crystals exhibit well-defined facets, indicating high crystallinity. For the solvoshaker method, the formation of both small and large particles with a wide range of sizes from 1.5 to 5 μm is observed. Additionally, the average crystal size inside the pores is 0.15 μm, indicating that HKUST-1 crystals are present inside the pores of PET TeMs as shown in Figure 3 for both the solvoshaker and solvothermal methods. Also, the difference between these two methods is the thickness of the HKUST-1 layer formed on the membrane surface: solvoshaker method: around 5 μm; solvothermal method: 11 μm. This also confirms the observations obtained with ATR-FTIR.

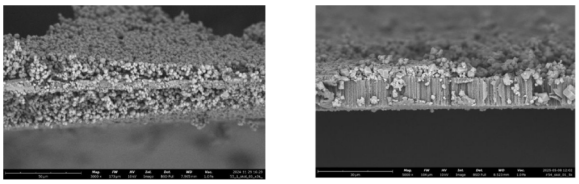

Figure 3. SEM images of the cross-section of PET TeMs_HKUST-1 solvothermal method (a) and solvoshaker method (b).

The SEM images in Figure 4 show the PET TeMs-Cu surface and after conversion to PET TeMs-$(CuOH)_2CO_3$. A change in the surface morphology and the formation of fluffy malachite crystals of various sizes, which are both on the surface and clogging the pores of the membrane, are clearly visible. The SEM images in Figure 5 show characteristic octahedral crystals typical of the HKUST-1 MOF structure on the surface of PET TeMs.[32] The octahedral crystals are evenly distributed across the substrate surface, with some of them forming aggregates. The well-defined crystal facets reflect the high degree of crystallinity of the HKUST-1 material. The crystal sizes of HKUST-1 obtained by the solvothermal method are more uniform and are around 2.6 μm, while HKUST-1 obtained by the solvoshaker method has a wider size distribution from 1.5 to 5 μm. The SEM results obtained in our study (Figures 3−5) were compared with previously published data on the morphology and structure of HKUST-1 (MOF-199) materials.[41−43] The average crystal sizes observed in our samples (∼2.6 μm on the surface and ∼0.15 μm inside the pores, solvothermal method) align well with those reported for HKUST-1 synthesized under comparable conditions.

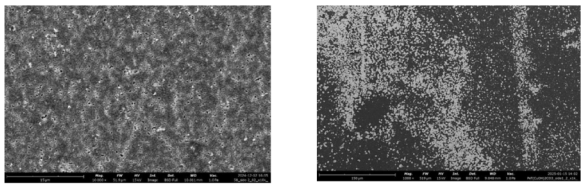

Figure 4. SEM analysis of the PET TeMs_Cu surface (a) and PET TeMs-$(CuOH)_2CO_3$ surface (b).

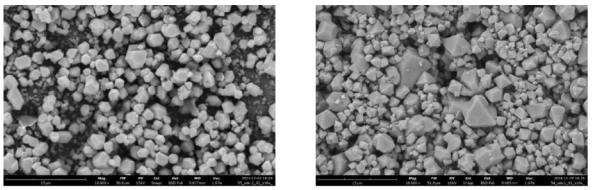

Figure 5. SEM image of the PET TeM_HKUST-1 surface solvothermal method (a) and solvoshaker method (b).

https://doi.org/10.1021/acsomega.5c01493
ACS Omega 2025, 10, 30259−30271

Table 2. EDX Analysis of the Samples

Sample	Atomic concentration, %			
	C	O	N	Cu
PET TeMs	80.24 ± 6.83	19.76 ± 3.21	-	-
PET TeMs_Cu	56.17 ± 5.21	25.52 ± 3.10	6.11 ± 1.52	12.20 ± 1.41
PET TeMs_-$(CuOH)_2CO_3$	39.42 ± 4.42	45.92 ± 3.45	-	14.66 ± 1.56
PET TeMs_HKUST-1 (solvothermal method)	56.02 ± 5.12	33.60 ± 3.54	4.46 ± 1.32	5.92 ± 0.56
PET TeMs_HKUST-1 (solvoshaker method)	42.07 ± 4.56	33.33 ± 3.11	17.22 ± 3.51	7.38 ± 0.43

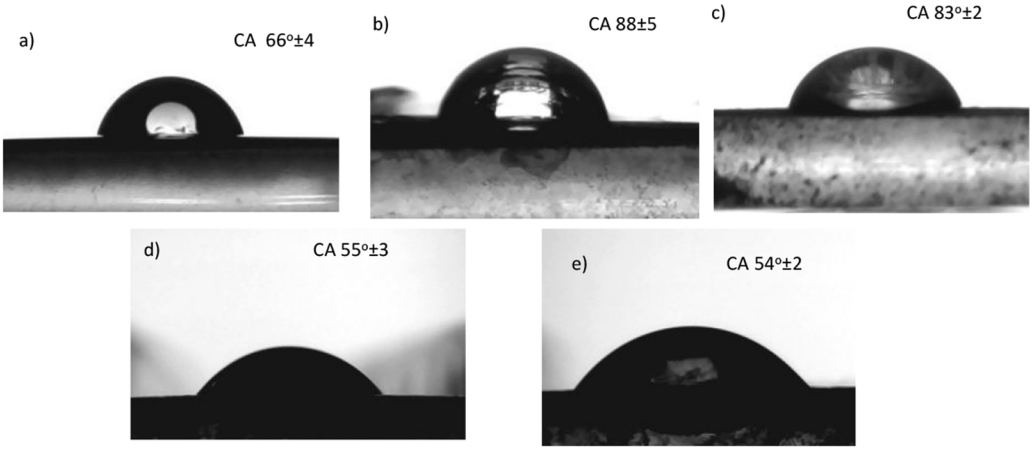

Figure 6. Contact angle (CA) of the original PET membrane (a), PET TeMs_Cu (b), PET TeMs_$(CuOH)_2CO_3$ (c), PET TeMs_HKUST-1 (solvothermal method) (d), and PET TeMs_HKUST-1 (solvoshaker method) (e).

The surface elemental composition of the samples was evaluated using EDX, and the atomic percentages of carbon (C), oxygen (O), nitrogen (N), and copper (Cu) are summarized in Table 2 (EDX spectra are presented in Figure S1, mapping on Figure S2). The PET TeMs exhibited a typical elemental distribution: carbon (80.24%) and oxygen (19.76%). After copper deposition, the copper signal (12.21%) was observed, and nitrogen (6.11%) appeared due to the presence of EDTA during the reaction. After the conversion of Cu to malachite, nitrogen was removed. The samples functionalized with HKUST-1 showed nitrogen and copper peaks due to the use of copper(II) nitrate as the metal precursor in both solvothermal and solvoshaker synthesis methods. Additionally, an unlabeled peak corresponding to gold (Au) was observed in all EDX spectra (at around 2.12 eV). This signal originates from the thin gold layer (~1.0−3.0 at. %) sputter-coated onto the membrane surfaces prior to analysis. The presence of gold was not quantified since it does not represent the actual membrane composition.

The contact angle (CA) was measured by using the static drop method, and the results are presented in Figure 6.

The oxidized surface of the PET TeMs exhibits a moderately hydrophobic character. CA of 66° indicates a certain degree of hydrophobicity. The deposited Cu (copper) coating demonstrates a CA of 88° higher than that of the oxidized PET membrane, indicating an increase in hydrophobicity. After treatment with $(CuOH)_2CO_3$ (malachite), the surface shows an average CA of 83°. This suggests that the surface retains hydrophobic properties similar to those of the copper coating; however, the slight reduction in the contact angle is likely due to the presence of polar groups. The film coated with HKUST-1 exhibits the lowest CA, ranging between 54° and 55°, indicating significant hydrophilicity. This result aligns with previous reports on HKUST-1.[44−46] Although no direct humidity tolerance tests were performed in this study, the observed contact angle suggests that the PET TeMs-HKUST-1 composite may exhibit reduced CO_2 sorption performance in high-humidity environments. Further studies are required to evaluate this behavior under the relevant operating conditions.

The surface area and pore size of the obtained samples were studied using nitrogen adsorption isotherms (77K). The results are presented in Table 3.

Table 3. Results of BET Analysis of the Samples

Sample	Specific area (m^2/g)	Langmuir Square (m^2/g)	Average pore size BJH, (nm)	Average pore volume BJH (cm^3/g)
PET TeMs	1.73	2.58	30.85	0.02
PET TeMs_Cu	9.25	17.68	17.66	0.07
PET TeMs_-$(CuOH)_2CO_3$	107.84	118.06	13.81	0.09
PET TeMs_HKUST-1 (solvothermal method)	382.76	517.98	15.57	0.37
PET TeMs_HKUST-1 (solvoshaker method)	99.31	142.68	9.82	0.04
HKUST-1	813.12	928.39	11.23	0.084

The BET analysis revealed a significant increase in specific surface area and pore volume as a result of the stepwise modification of PET TeMs. The pristine PET TeMs exhibited a low specific surface area of 1.73 m^2/g. Upon modification with copper deposition (PET TeMs_Cu) and subsequent conversion to the malachite phase (PET TeMs_-$(CuOH)_2CO_3$), the surface area increased substantially to 107.84 m^2/g. The growth of HKUST-1 on the membranes via

https://doi.org/10.1021/acsomega.5c01493
ACS Omega 2025, 10, 30259−30271

the solvothermal method resulted in a further increase in the surface area to 382.76 m^2/g and a pore volume of 0.37 cm^3/g. In contrast, the solvoshaker method led to a surface area of 99.31 m^2/g suggesting that the solvothermal method is more effective for growing a thick (which also comes from SEM images and FTIR-ATR) MOF layer under elevated temperature and pressure conditions. These differences may be attributed to the improved nucleation and crystallinity of HKUST-1 in solvothermal conditions compared to the less intense solvoshaker approach. Regarding initial HKUST-1 powder, surface area of 813.12 m^2/g can be comparted previously reported data in the literature,[47,48] where HKUST-1 surface areas typically range from 700 to over 1200 m^2/g, depending on synthesis conditions, solvent system, activation method, and crystallinity.

Figure 8 presents the XRD patterns of the studied samples obtained at room temperature. A powder diffractogram of the HKUST-1 material, previously synthesized by the hydrothermal method in powder form, was used as a reference. The phase composition was determined using the PDF database. For comparison purposes, the PDF card of the HKUST-1 material (PDF 00-065-1028, space group $Fm\bar{3}m$) is also provided. Phase analysis based on the recorded diffractograms for the PET membrane samples with HKUST-1 (solvoshaker, solvothermal) shows that the films contain phases of PET and HKUST-1. This is evidenced by the intense reflections of PET (100), (110), (2−30) and the reflections of HKUST-1 (222), (220), (111), (400), and others. The positions of the reflections in the composite samples and the powder phase of HKUST-1 remain unchanged, indicating identical lattice parameters and interplanar spacings. For the PET membrane sample with copper (Cu), the presence of a (111) reflection from the copper phase with a face-centered cubic lattice is noted.

The XRD results presented in Figure 7 were compared with the published XRD patterns of MOF-199 and HKUST-1, as shown in the studies.[41,43,49] The characteristic diffraction peaks observed in our samples (including the PET_TeMs_HKUST-1 samples synthesized via solvoshaker and solvothermal methods) match well with those of the hydrothermally synthesized HKUST-1 powder and the reference PDF card. This confirms the successful formation of the HKUST-1 phase with consistent lattice parameters and interplanar spacings across all synthesized materials. In addition, the PET_TeMs_-Cu sample exhibits a peak corresponding to the (111) reflection of metallic copper, consistent with standard copper XRD patterns, which is also compared with previous studies.[50,51] These comparisons further validate the structural identity and crystalline quality of the synthesized HKUST-1.

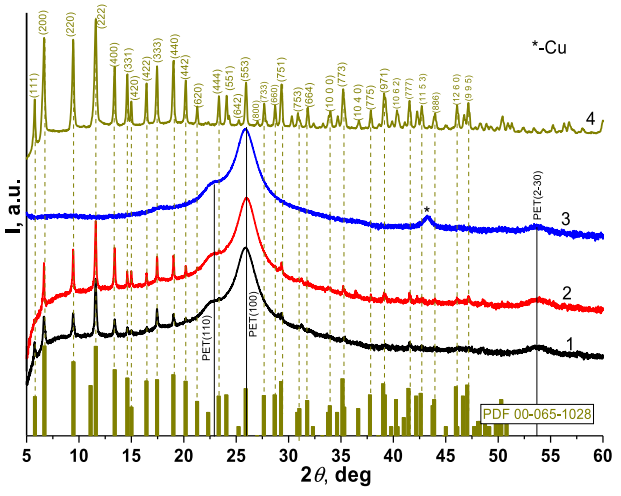

Figure 7. Comparison of XRD of representative samples and the PDF card of the HKUST-1 crystalline phase. 1: PET TeMs_HKUST-1 sample (solvoshaker method), 2: PET TeMs_HKUST-1 sample (solvothermal method), 3: PET TeMs_Cu sample, and 4: HKUST-1 synthesized by the hydrothermal method in powder form.

Figure 8a−f presents the thermograms of PET TeMs, HKUST-1, membranes with Cu, $(CuOH)_2CO_3$, and HKUST-1 synthesized using solvothermal and solvoshaker methods. The single-stage weight loss of copper containing samples shows multistage degradation upon the inclusion of MOFs.

In Figure 8a, the sample's mass remains stable up to 300 °C, indicating the absence of significant decomposition processes. Between 300 and 400 °C, a decrease in mass is observed on the TG curve, marking the initial stage of polymer (PET) thermal decomposition. Between 400 and 500 °C, a sharp mass loss of 79.9% occurs, indicating active decomposition of organic components. From 500 to 800 °C, the mass remains nearly constant after the decomposition is complete. The residual mass (∼25−30%) is attributed to the presence of inorganic remnants, in this case, copper (Cu) or its oxides (CuO). The single-step nature of the decomposition curve indicates that the main decomposition process occurs within a relatively narrow temperature range. A very similar behavior has been observed for PET TeMs containing $(CuOH)_2CO_3$ as indicated in Figure 8b. While the thermograms of the PET TeMs-Cu and PET TeMs-malachite samples are very similar, they show significant changes for the PET TeMs-HKUST-1 samples.

In Figure 8c,e,f, all samples exhibit a multistep decomposition occurring in the range of 250−400 °C, which are quite similar to those of HKUST-1. The first mass loss is associated with the removal of physically adsorbed water and part of the solvent from the pores. The second and third mass losses correspond to the step destruction of the organic ligand (trimesic acid). Finally, the last mass loss corresponds to the breaking of PET polymer chains, as shown in Figure 9d, which shows the typical mass loss of PET_TeMs after 400 °C.[52] The differences between the synthesis methods (solvoshaker and solvothermal) are reflected in the intensity and overall mass loss.

3.2. CO_2 Capture by PET TeMs-HKUST-1. Uptake and release of CO_2 by the composite membranes were performed by following the procedure described in Section 2.5. Membranes with immobilized HKUST-1 were used for CO_2 sorption/desorption analysis via TGA.[53,54] The graph in Figure 9 demonstrates 12 distinct cycles of CO_2 sorption−desorption that was performed during more than 20 h. The amplitude of the mass change remains stable, confirming the sustainability of the sorbent material over multiple uses. The CO_2 absorption process, which took 60 min, is accompanied by an increase in mass. After absorption was completed, heating of the samples to 150 °C started, and a decrease in mass was observed, indicating CO_2 desorption in 60 min. The mass changes fluctuate between 97−118% (solvothermal) and 92−118% (solvoshaker) relative to the first cycle, demonstrating the reproducibility of the sorption−desorption cycles and the stability of the membranes with HKUST-1.

https://doi.org/10.1021/acsomega.5c01493
ACS Omega 2025, 10, 30259−30271

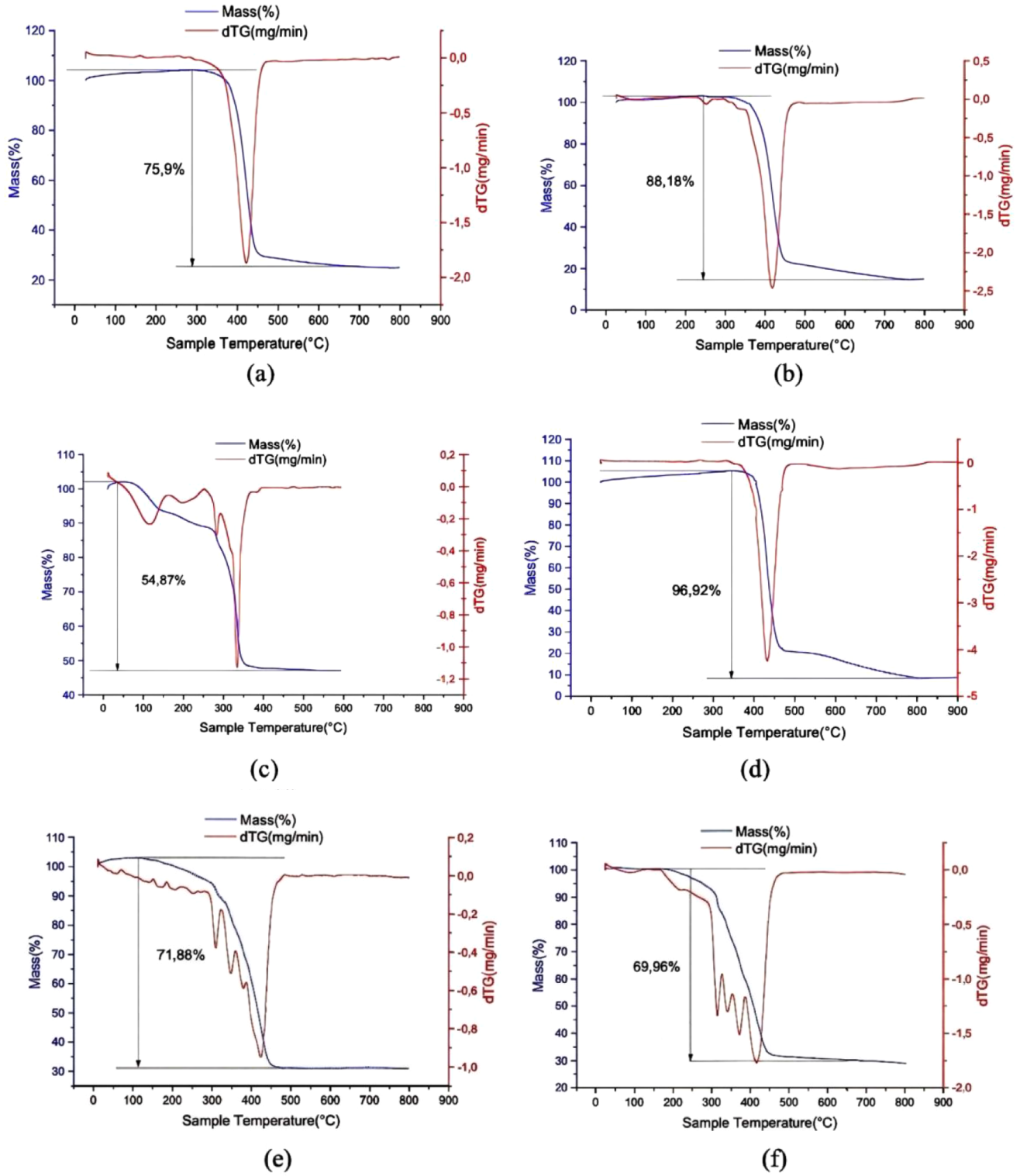

Figure 8. Thermogravimetric analysis results of the samples: (a) PET TeMs_Cu, (b) PET TeMs_$(CuOH)_2CO_3$, (c) HKUST-1, (d) PET_TeMs, (e) PET TeMs_HKUST-1 (solvoshaker method), and (f) PET TeMs_HKUST-1 (solvothermal method).

The adsorption capacity (AC) was calculated by using the following equation:

$$AC = \frac{m_1/44.009}{m_0}$$

AC − adsorption capacity, mmol/g
m_0 − mass of the membrane, g
44.009 − molar mass of CO_2, mg/mmol
m_1 − mass of adsorbed CO_2, mg

Figure 10 illustrates the adsorption capacity of PET TeMs-HKUST-1 materials synthesized using two different methods: solvoshaker (black bars) and solvothermal (red bars) over 12 adsorption−desorption cycles. The average adsorption capacity for PET TeMs-HKUST-1 prepared using the

https://doi.org/10.1021/acsomega.5c01493
ACS Omega 2025, 10, 30259−30271

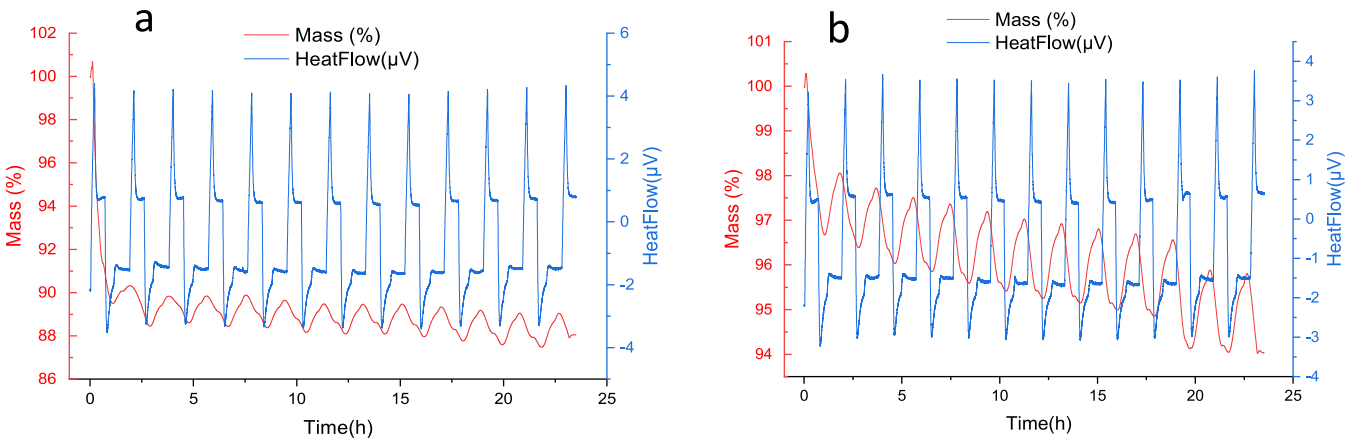

Figure 9. Results of 12 sorption−desorption cycles of PET TeMs_HKUST-1 samples: solvoshaker method (a) and solvothermal method (b).

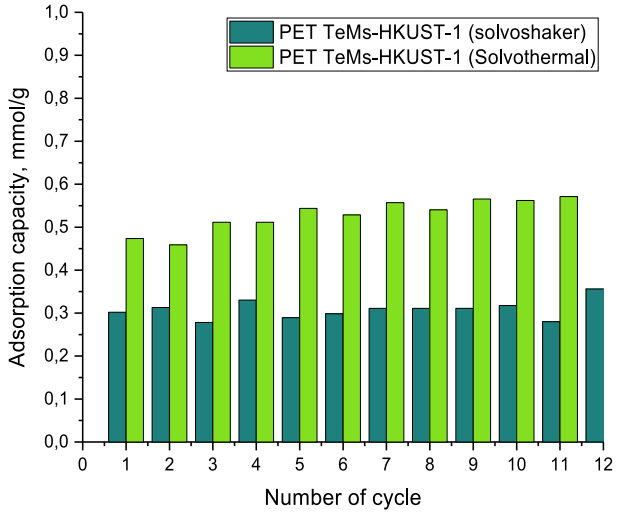

Figure 10. Results of the adsorption capacity of PET membranes with HKUST-1 obtained by solvoshaker method and solvothermal method at 12 cycles.

solvothermal method is 0.53 ± 0.03 mmol/g, while that obtained via the solvoshaker method is 0.31 ± 0.02 mmol/g. Throughout the 12 cycles, both samples maintain relatively stable performance, with fluctuations in adsorption capacity remaining within 97−118% (solvothermal) and 92−117% (solvoshaker) relative to the first cycle. This indicates good reusability and structural stability of the composites under repeated use conditions.

The observed differences between the synthesis methods suggest a more efficient sorption−desorption performance for the samples obtained via the solvothermal method. This enhanced efficiency can be attributed to their larger specific surface area, as confirmed by BET analysis, and the greater thickness of the HKUST-1 layer, as revealed by SEM imaging.

In order to evaluate the selectivity of the CO_2 sorption in relation to the N_2 sorption, gravimetric TGA was also estimated. The adsorption capacity of PET TeMs-HKUST-1 (solvoshaker methods) is 0.099 ± 0.015 mmol/g (1 h of adsorption), while that of PET TeMs-HKUST-1 (solvothermal methods) is 0.102 ± 0.012 mmol/g (1 h of adsorption). Thus, the ratio of the adsorption capacity of CO_2 to the adsorption capacity of N_2 is 3.1 for the solvoshaker method and 5.2 for the solvothermal method, which demonstrates the dominant sorption of carbon dioxide compared to nitrogen. However, it should be noted that more accurate measurements of selectivity on real gas mixtures or using the IAST theory are required.

The CO_2 adsorption performance of PET TeMs-HKUST-1 is influenced by the method of HKUST-1 synthesis. The method of synthesis affects both the morphology of HKUST-1 and its concentration on the surface and inside the pores of

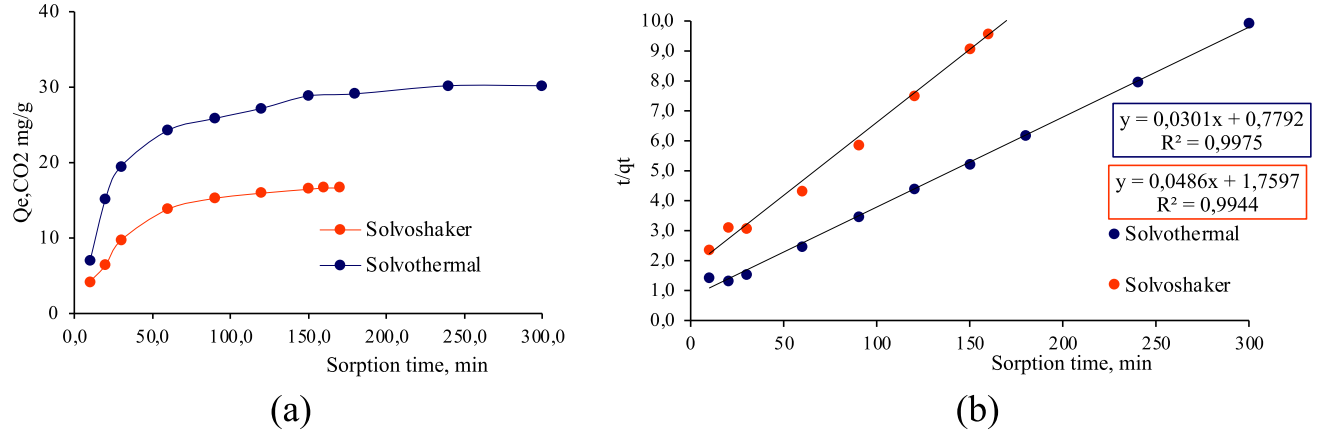

Figure 11. Adsorption kinetic for CO_2 for PET TeMs-HKUST-1 solvoshaker and solvothermal methods (a) and linearized pseudo-second-order kinetic model for CO_2 adsorption (b).

https://doi.org/10.1021/acsomega.5c01493
ACS Omega 2025, 10, 30259−30271

Table 4. The CO_2 Adsorption Capacities Obtained in Our Study and in Selected Works

Study	Pressure (bar)	Temperature (°C)	Material	Adsorption capacity (mmol/g)	Regeneration	Notes
This study (solvoshaker method)	1	25	PET TeMs-HKUST-1	0.31 (1 h) 0.38 (5 h)	12 cycles	High cycling stability
This study (solvothermal method)	1	25	PET TeMs-HKUST-1	0.53 (1 h) 0.69 (5 h)	12 cycles	High cycling stability
Shang et al. (2020)[58]	1	25	GO/HKUST-1 composite	1.526	Not reported	Graphene oxide-based material
Zhao et al. (2014)[59]	5	32	HKUST-1 at atmospheric pressure	1.8	Not reported	Moderate adsorption at 32 °C
Mu et al. (2018)[34]	1	27	HKUST-1 1 (nanoscale, mild conditions)	1.84	Not reported	Smaller particle size improves performance
Ho et al. (2022)[33]	1	30	Solvent-free HKUST-1	1.7	5 cycles	Green synthesis approach
Mu et al. (2018)[34]	1	27	GO/HKUST-1 composite	2.5	Not reported	increased surface area and improved hydrophilicity
Girimonte et al. (2024)[60]	1	-	Ceramic foams/HKUST-1	0.4	Not reported	Sustainability, regenerative cycling, scalability
Fateminia et al. (2023)[61]	0,82	27	core/shell Nylon 6,6/La-TMA	0.219	Not reported	MOF-shell nanocomposite fiber obtained by coaxial electrospinning
Sneddon et al. (2017)[62]	Not reported	30	EDA−PVC/SBA-15	0.54	Not reported	1:1 CO_2/N_2 mixtures; full regeneration at 75 °C

PET TeMs. From the SEM images presented in Figures 3 and 5, it is seen that the solvoshaker method led to the presence of smaller crystals (and also together with large ones) in comparison to the solvothermal method. Moreover, a key morphological factor affecting the CO_2 sorption is crystal coverage. As seen in the SEM images, solvothermal synthesis produces a more continuous thick HKUST-1 layer (mass increase is 18.56%), potentially reducing accessibility to deeper sorption sites within the membrane. In contrast, solvoshaker synthesis results in a thinner layer of HKUST-1 (mass increase is 7.75%). These differences explain why solvothermal-synthesized membranes exhibited a higher initial CO_2 adsorption capacity (0.53 mmol/g) compared to solvoshaker samples (0.31 mmol/g) after 1 h of adsorption.

Figure 11a illustrates the kinetic profiles of CO_2 adsorption on PET TeMs-HKUST-1 composites synthesized by using solvothermal and solvoshaker methods. The adsorption capacity is plotted as a function of contact time up to 300 min for the solvothermal method and up to 170 min for the solvoshaker method (since above 170 min saturation occurred and the adsorption capacity did not increase up to 300 min). Both materials exhibit a typical two-phase kinetic behavior: a rapid initial uptake followed by a slower approach to equilibrium.

The solvothermal sample demonstrates a significantly higher adsorption capacity, reaching approximately 30.2 mg/g (0.69 mmol/g) after 5 h of sorption, while the solvoshaker sample plateaus at around 16.7 mg/g (0.38 mmol/g). Figure 11b presents the linearized form of the pseudo-second-order kinetic model for the adsorption of CO_2 for both samples. The plots display the relationship between t/q_t and sorption time t, allowing the determination of kinetic parameters.

Both methods show a strong linear correlation with high regression coefficients: R^2 = 0.9975 for the solvothermal sample and R^2 = 0.9944 for the solvoshaker sample, confirming the applicability of the pseudo-second-order model. The slope and intercept of the fitted lines were used to calculate the equilibrium adsorption capacity q_e and the pseudo-second-order rate constant k_2. The solvothermal method showed an adsorption capacity q_e = 33.22 mg/g and a rate constant k_2 = 1.16×10^{-3} g/(mg·min). The solvoshaker sample yielded a lower capacity (q_e = 20.58 mg/g) and a higher rate constant (k_2 = 1.34×10^{-3} g/(mg·min)) in comparison with the solvothermal method. These findings indicate that while the solvoshaker method provides a little faster kinetics, the solvothermal approach ensures a higher sorption capacity, due to the improved structural properties of the composite, as was mentioned above.

Recent studies have explored various strategies to enhance the CO_2 sorption capacity and stability of HKUST-1-based materials. For example, HKUST-1 composites incorporating pyrolyzed byproducts demonstrated improved water stability and CO_2 adsorption efficiency.[55] Similarly, graphene oxide (GO)-modified HKUST-1 exhibited enhanced CO_2 uptake due to increased surface area and improved hydrophilicity.[56] Another study focused on HKUST-1 templated with polyethylene glycol, leading to an unusually large microporous structure that enhanced CO_2 and CH_4 separation performance.[9,57] Additionally, a one-step hydrothermal synthesis of monolithic HKUST-1 was developed to simplify the fabrication process while maintaining high adsorption efficiency.[57] To evaluate the efficiency of the synthesized PET TeMs-HKUST-1 composites, we compared our results to previously reported CO_2 adsorption capacities of similar MOF-based materials (Table 4).

These findings suggest that PET TeMs-HKUST-1 composite membranes synthesized via the solvoshaker method offer a competitive alternative to existing MOF-based materials, combining high adsorption efficiency, scalability, and energy efficiency. Future research should focus on optimizing reaction conditions to further enhance MOF adhesion and crystallinity, thereby improving material performance, as well as conducting research on the selectivity of CO_2 separation in relation to other gases.

4. CONCLUSIONS

This study successfully demonstrates the synthesis of HKUST-1 on PET track-etched membranes by using solvothermal and solvoshaker methods. The immobilization of HKUST-1 on PET membranes resulted in composite materials with high

https://doi.org/10.1021/acsomega.5c01493
ACS Omega 2025, 10, 30259−30271

crystallinity and good sorption properties. SEM analysis confirmed the formation of uniform octahedral HKUST-1 crystals, evenly distributed across the membrane surface as well as inside the channels of the membrane. XRD analysis further validated the integrity of the crystalline structure, while BET measurements revealed a significant surface area enhancement compared with uncoated PET membranes.

In this work, sorption studies highlighted the CO_2 adsorption and regeneration performance of these composites. The solvoshaker method achieved stable adsorption capacities at 0.31 ± 0.02 mmol/g (1 h of adsorption), and the solvothermal method exhibited an adsorption capacity of 0.53 ± 0.03 mmol/g (1 h of adsorption) with high regeneration efficiency after 12 cycles of sorption−desorption, indicating excellent cycling stability. These results underscore the material's durability and effectiveness in repeated CO_2 capture cycles. Overall, the synthesized PET TeMs-HKUST-1 composites represent a promising solution for scalable CO_2 capture, combining the advantages of metal−organic frameworks with the structural flexibility and stability of polymer membranes.

■ ASSOCIATED CONTENT

Supporting Information

The Supporting Information is available free of charge at https://pubs.acs.org/doi/10.1021/acsomega.5c01493.

EDX spectra of the samples and mapping from EDX analysis (PDF)

■ AUTHOR INFORMATION

Corresponding Author

Ilya V. Korolkov − *The Institute of Nuclear Physics, Almaty 050032, Kazakhstan; L.N. Gumilyov Eurasian National University, Astana 010008, Kazakhstan;* orcid.org/0000-0002-0766-2803; Email: i.korolkov@inp.kz

Authors

Dias D. Omertassov − *The Institute of Nuclear Physics, Almaty 050032, Kazakhstan; L.N. Gumilyov Eurasian National University, Astana 010008, Kazakhstan*

Aigerim Kh. Shakayeva − *The Institute of Nuclear Physics, Almaty 050032, Kazakhstan; L.N. Gumilyov Eurasian National University, Astana 010008, Kazakhstan*

Zhanna K. Zhatkanbayeva − *L.N. Gumilyov Eurasian National University, Astana 010008, Kazakhstan*

Rafael I. Shakirzyanov − *L.N. Gumilyov Eurasian National University, Astana 010008, Kazakhstan;* orcid.org/0000-0001-9908-3034

Maxim V. Zdorovets − *The Institute of Nuclear Physics, Almaty 050032, Kazakhstan; L.N. Gumilyov Eurasian National University, Astana 010008, Kazakhstan*

Olgun Güven − *Department of Chemistry, Hacettepe University, Ankara 06800, Turkey*

Complete contact information is available at: https://pubs.acs.org/10.1021/acsomega.5c01493

Author Contributions

D.D.O.: Investigation, methodology, validation, writing—original draft. A.K.S.: Investigation, methodology, validation, writing—original draft. Z.K.Z.: Supervision, writing—review and editing. R.I.S.: Investigation, data curation. M.V.Z.: Supervision, data curation. O.G.: Conceptualization, supervision, writing—review and editing. I.V.K.: Conceptualization, supervision, writing—review and editing, project administration, funding acquisition.

Funding

The work was carried out with the financial support of the Ministry of Science and Higher Education of the Republic of Kazakhstan (Grant No. AP19676702).

Notes

The authors declare no competing financial interest.

■ ACKNOWLEDGMENTS

Artificial intelligence-based tools were utilized to assist in the grammatical and stylistic review of the manuscript. The initial draft of the manuscript and its further modifications were written by the authors themselves, and after using the software, the authors additionally reviewed and edited the output and took full responsibility for the content of this publication.

■ REFERENCES

(1) Song, C. Global Challenges and Strategies for Control, Conversion and Utilization of CO2 for Sustainable Development Involving Energy, Catalysis, Adsorption and Chemical Processing. *Catal. Today* **2006**, *115* (1−4), 2−32.

(2) Melillo, J. M.; McGuire, A. D.; Kicklighter, D. W.; Moore, B.; Vorosmarty, C. J.; Schloss, A. L. Global Climate Change and Terrestrial Net Primary Production. *Nature* **1993**, *363* (6426), 234−240.

(3) Levin, S. A. The Problem of Pattern and Scale in Ecology: The Robert H. MacArthur Award Lecture. *Ecology* **1992**, *73* (6), 1943−1967.

(4) Dorozhkina, I. P.; Cherepovitsyna, A. A. Complex Of Technologies For Carbon Capture, Utilization And Storage: Theory And Practice Of Organizational Forms Of Implementation. *Models, Systems, Networks In Economics, Technology, Nature And Society* **2023**, *3*, 38−52.

(5) Gough, C. Carbon Capture and Its Storage: An Integrated Assessment. In *Carbon Capture And Its Storage*, 1st ed.; Shackley, S., Ed.; Routledge, 2016. DOI: .

(6) Güven, O.; Han, B. S. The Prospects for Radiation Technology in Mitigating Carbon Footprint. *Radiat. Phys. Chem.* **2022**, *198*, 110282.

(7) Mangal, S.; Shanmuga Priya, S. Metal-Organic Frameworks for Carbon Dioxide Capture. In *Sustainable Agriculture Reviews 38*, Inamuddin, Asiri, A., Lichtfouse, E., Eds.; Springer: Cham, 2019; pp. 169−191.

(8) Choi, S.; Drese, J. H.; Jones, C. W. Adsorbent Materials for Carbon Dioxide Capture from Large Anthropogenic Point Sources. *ChemSuschem* **2009**, *2* (9), 796−854.

(9) Aloufi, F. A.; Missaoui, N.; Halawani, R. F.; Kahri, H.; Jamoussi, B.; Gross, A. J. Unusually Large Microporous HKUST-1 via Polyethylene Glycol-Templated Synthesis: Enhanced CO2 Uptake with High Selectivity over CH4 and N2. *Environ. Sci. Pollut. Res.* **2024**, *31* (21), 31355−31372.

(10) Decoste, J. B.; Peterson, G. W. Metal-Organic Frameworks for Air Purification of Toxic Chemicals. *Chem. Rev.* **2014**, *114* (11), 5695−5727.

(11) Li, J. R.; Kuppler, R. J.; Zhou, H. C. Selective Gas Adsorption and Separation in Metal-Organic Frameworks. *Chem. Soc. Rev.* **2009**, *38* (5), 1477−1504.

(12) James, S. L. Metal-Organic Frameworks. *Chem. Soc. Rev.* **2003**, *32* (5), 276−288.

(13) Rowsell, J. L. C.; Yaghi, O. M. Metal-Organic Frameworks: A New Class of Porous Materials. *Microporous Mesoporous Mater.* **2004**, *73* (1−2), 3−14.

(14) Chen, C.; Lee, Y. R.; Ahn, W. S. CO2 Adsorption over Metal-Organic Frameworks: A Mini Review. *J. Nanosci. Nanotechnol.* **2016**, *16* (5), 4291−4301.
(15) Zheng, Z.; Rampal, N.; Inizan, T. J.; Borgs, C.; Chayes, J. T.; Yaghi, O. M. Large Language Models for Reticular Chemistry. *Nat. Rev. Mater.* **2025**, *10*, 369−381.
(16) Furukawa, H.; Cordova, K. E.; O'Keeffe, M.; Yaghi, O. M. The Chemistry and Applications of Metal-Organic Frameworks. *Science* **2013**, *341* (6149), 1230444.
(17) Butova, V. V.; Soldatov, M. A.; Guda, A. A.; Lomachenko, K. A.; Lamberti, C. Metal-Organic Frameworks: Structure, Properties, Methods of Synthesis and Characterization. *Russ. Chem. Rev.* **2016**, *85* (3), 280−307.
(18) Lee, J.; Farha, O. K.; Roberts, J.; Scheidt, K. A.; Nguyen, S. T.; Hupp, J. T. Metal-Organic Framework Materials as Catalysts. *Chem. Soc. Rev.* **2009**, *38* (5), 1450−1459.
(19) Akeremale, O. K.; Ore, O. T.; Bayode, A. A.; Badamasi, H.; Adedeji Olusola, J.; Durodola, S. S. S. Characterization, and Activation of Metal Organic Frameworks (MOFs) for the Removal of Emerging Organic Contaminants through the Adsorption-Oriented Process: A Review. *Results Chem.* **2023**, *5*, 100866.
(20) Zhao, X.; Wang, Y.; Li, D. S.; Bu, X.; Feng, P. Metal−Organic Frameworks for Separation. *Adv. Mater.* **2018**, *30* (37), 1705189.
(21) Yañez-Aulestia, A.; Trejos, V. M.; Esparza-Schulz, J. M.; Ibarra, I. A.; Sánchez-González, E. Chemically Modified HKUST-1(Cu) for Gas Adsorption and Separation: Mixed-Metal and Hierarchical Porosity. *ACS Appl. Mater. Interfaces* **2024**, *16*, 65581−65591.
(22) Abraham, D. S.; Athul, K. V.; Shamna, I.; Bhagiyalakshmi, M.; Jeong, S. K. Rationalizing the Efficiency of HKUST-1 for Capture and Biomimetic Sequestration of CO2. *Korean J. Chem. Eng.* **2024**, *41* (5), 1467−1478.
(23) Korolkov, I. V.; Narmukhamedova, A. R.; Melnikova, G. B.; Muslimova, I. B.; Yeszhanov, A. B.; Zhatkanbayeva, Z. K.; Chizhik, S. A.; Zdorovets, M. V. Preparation of Hydrophobic PET Track-Etched Membranes for Separation of Oil−Water Emulsion. *Membranes* **2021**, *11* (8), 637.
(24) Apel, P. Track Etching Technique in Membrane Technology. *Radiat. Meas.* **2001**, *34* (1−6), 559−566.
(25) Shakayeva, A. K.; Yeszhanov, A. B.; Zhumazhanova, A. T.; Korolkov, I. V.; Zdorovets, M. V. Fabrication of Hydrophobic PET Track-Etched Membranes Using 2,2,3,3,4,4,4-Heptafluorobutyl Methacrylate for Water Desalination by Membrane Distillation. *Eurasian J. Chem.* **2024**, *29* (2 (114)), 81−88.
(26) Yeszhanov, A. B.; Korolkov, I. V.; Kh Shakayeva, A. K.; Lissovskaya, L. I.; Zdorovets, M. V. Preparation of Poly(Ethylene Terephthalate) Track-Etched Membranes for the Separation of Water-Oil Emulsions. *Eurasian J. Chem.* **2023**, *110* (2), 131−138.
(27) Korolkov, I. V.; Mashentseva, A. A.; Güven, O.; Gorin, Y. G.; Kozlovskiy, A. L.; Zdorovets, M. V.; Zhidkov, I. S.; Cholach, S. O. Electron/Gamma Radiation-Induced Synthesis and Catalytic Activity of Gold Nanoparticles Supported on Track-Etched Poly(Ethylene Terephthalate) Membranes. *Mater. Chem. Phys.* **2018**, *217*, 31−39.
(28) Korolkov, I. V.; Güven, O.; Mashentseva, A. A.; Atıcı, A. B.; Gorin, Y. G.; Zdorovets, M. V.; Taltenov, A. A. Radiation Induced Deposition of Copper Nanoparticles inside the Nanochannels of Poly(Acrylic Acid)-Grafted Poly(Ethylene Terephthalate) Track-Etched Membranes. *Radiat. Phys. Chem.* **2017**, *130*, 480−487.
(29) Parmanbek, N.; Sütekin, D. S.; Barsbay, M.; Mashentseva, A. A.; Zheltov, D. A.; Aimanova, N. A.; Jakupova, Z. Y.; Zdorovets, M. V. Hybrid PET Track-Etched Membranes Grafted by Well-Defined Poly(2-(Dimethylamino)Ethyl Methacrylate) Brushes and Loaded with Silver Nanoparticles for the Removal of As(III). *Polymers* **2022**, *14* (19), 4026.
(30) Aimanova, N. A.; Almanov, A. A.; Alipoori, S.; Barsbay, M.; Zhumabayev, A. M.; Nurpeisova, D. T.; Mashentseva, A. A. Development of the All-Solid-State Flexible Supercapacitor Membranes via RAFT-Mediated Grafting and Electrospun Nanofiber Modification of Track-Etched Membranes. *RSC Adv.* **2025**, *15* (8), 6260−6280.
(31) Usman, M.; Ali, M.; Al-Maythalony, B. A.; Ghanem, A. S.; Saadi, O. W.; Ali, M.; Jafar Mazumder, M. A.; Abdel-Azeim, S.; Habib, M. A.; Yamani, Z. H.; et al. Highly Efficient Permeation and Separation of Gases with Metal-Organic Frameworks Confined in Polymeric Nanochannels. *ACS Appl. Mater. Interfaces* **2020**, *12* (44), 49992−50001.
(32) Lestari, W. W.; Adreane, M.; Purnawan, C.; Fansuri, H.; Widiastuti, N.; Rahardjo, S. B. Solvothermal and Electrochemical Synthetic Method of HKUST-1 and Its Methane Storage Capacity. In *IOP Conference Series: Materials Science and Engineering*, IOP Publishing, 2016; Vol: *107*(1); p. 012030. DOI: .
(33) Ho, P. S.; Chong, K. C.; Lai, S. O.; Lee, S. S.; Lau, W. J.; Lu, S. Y.; Ooi, B. S. Synthesis of Cu-BTC Metal-Organic Framework for CO2 Capture via Solvent-Free Method: Effect of Metal Precursor and Molar Ratio. *Aerosol Air Qual. Res.* **2022**, *22* (12), 220235.
(34) Mu, X.; Chen, Y.; Lester, E.; Wu, T. Optimized Synthesis of Nano-Scale High Quality HKUST-1 under Mild Conditions and Its Application in CO2 Capture. *Microporous Mesoporous Mater.* **2018**, *270*, 249−257.
(35) Korolkov, I. V.; Mashentseva, A. A.; Güven, O.; Niyazova, D. T.; Barsbay, M.; Zdorovets, M. V. The Effect of Oxidizing Agents/Systems on the Properties of Track-Etched PET Membranes. *Polym. Degrad. Stab.* **2014**, *107*, 150−157.
(36) Korolkov, I. V.; Borgekov, D. B.; Mashentseva, A. A.; Güven, O.; Atlcl, A. B.; Kozlovskiy, A. L.; Zdorovets, M. V. The Effect of Oxidation Pretreatment of Polymer Template on the Formation and Catalytic Activity of Au/PET Membrane Composites. *Chem. Pap.* **2017**, *71* (12), 2353−2358.
(37) Altynbaeva, L. S.; Mashentseva, A. A.; Aimanova, N. A.; Zheltov, D. A.; Shlimas, D. I.; Nurpeisova, D. T.; Barsbay, M.; Abuova, F. U.; Zdorovets, M. V. Eco-Friendly Electroless Template Synthesis of Cu-Based Composite Track-Etched Membranes for Sorption Removal of Lead(II) Ions. *Membranes* **2023**, *13* (5), 495.
(38) Du, J.; Zhou, C.; Yang, Z.; Cheng, J.; Shen, Y.; Zeng, X.; Tan, L.; Dong, L. Conversion of Solid Cu2(OH)2CO3 into HKUST-1 Metal-Organic Frameworks: Toward an under-Liquid Superamphiphobic Surface. *Surf. Coat. Technol.* **2019**, *363*, 282−290.
(39) Isaeva, V. I.; Barkova, M. I.; Kucherov, A. V.; Ermilova, M. M.; Orekhova, E. V.; Kustov, L. M.; Yaroslavtsev, A. B. Preparation of Composite Membranes on a Ceramic Base with Supported Metal-Organic Framework Structure of MOF-199 and Study of Their Adsorption Properties. *Nanotechnol. Russ.* **2014**, *9* (7−8), 416−422.
(40) Loera-Serna, S.; Solis, H.; Ortiz, E.; Martínez-Hernandéz, A. L.; Noreña, L. Elimination of Methylene Blue and Reactive Black 5 from Aqueous Solution Using HKUST-1. *Int. J. Environ. Sci. Dev.* **2017**, *8* (4), 241−246.
(41) Thi, T. V. N.; Luu, C. L.; Hoang, T. C.; Nguyen, T.; Bui, T. H.; Nguyen, P. H. D.; Thi, T. P. P. Synthesis of MOF-199 and Application to CO2 Adsorption. *Adv. Nat. Sci.: Nanosci. Nanotechnol.* **2013**, *4* (3), 035016.
(42) Sulistiono, D. O.; Santoso, E.; Ediati, R. Enhanced Adsorption of Methylene Blue and Congo Red from Aqueous Solutions by MCM-41/HKUST-1 Composites. *Asian J. Chem.* **2019**, *31* (8), 1675−1682.
(43) Biemmi, E.; Christian, S.; Stock, N.; Bein, T. High-Throughput Screening of Synthesis Parameters in the Formation of the Metal-Organic Frameworks MOF-5 and HKUST-1. *Microporous Mesoporous Mater.* **2009**, *117* (1−2), 111−117.
(44) Sran, B. S.; Lee, E. W.; Yoon, J. W.; Jo, D.; Cho, K. H.; Lee, S. K.; Lee, U. H. Selective Adsorption of Acetylene over Carbon Dioxide on Glycine Functionalized HKUST-1 with Enhanced Moisture Stability. *Sep. Purif. Technol.* **2024**, *328*, 124939.
(45) Kuchekar, S.; Gaikwad, S.; Han, S. Design and Synthesis of Mg-HKUST-1/Solid Ionic Liquid Composites for CO2 Capture with Improved Water Stability. *J. Environ. Chem. Eng.* **2024**, *12* (5), 113379.
(46) Liu, Z.; Yang, S.; Wang, Z.; Ji, N.; Li, X.; Zuo, Y. Construction of Hydrophobic HKUST-1 in Wood with Selective Adsorption

Performance for Toluene and Moisture Blends. *Sep. Purif. Technol.* **2025**, *357*, 130134.
(47) Sahiner, N.; Sel, K.; Ozturk, O. F.; Demirci, S.; Terzi, G. Facile Synthesis and Characterization of Trimesic Acid-Cu Based Metal Organic Frameworks. *Appl. Surf. Sci.* **2014**, *314*, 663−669.
(48) Samuel, M. S.; Savunthari, K. V.; Ethiraj, S. Synthesis of a Copper (II) Metal−Organic Framework for Photocatalytic Degradation of Rhodamine B Dye in Water. *Environ. Sci. Pollut. Res.* **2021**, *28* (30), 40835−40843.
(49) Li, Y.; Yang, R. T. Hydrogen Storage in Metal-Organic and Covalent-Organic Frameworks by Spillover. *AIChE J.* **2008**, *54* (1), 269−279.
(50) Phul, R.; Kaur, C.; Farooq, U.; Ahmad, T. Ascorbic Acid Assisted Synthesis, Characterization and Catalytic Application of Copper Nanoparticles. *Mater. Sci. Eng. Int. J.* **2018**, *2* (4), 90−94.
(51) Nasirian, A. Synthesis and Characterization of Cu Nanoparticles and Studying of Their Catalytic Properties. *Int. J. Nano Dimens.* **2012**, *2* (3), 159−164.
(52) Tian, F.; Qiao, C.; Zheng, R.; Ru, Q.; Sun, X.; Zhang, Y.; Meng, C. Synthesis of Bimetallic-Organic Framework Cu/Co-BTC and the Improved Performance of Thiophene Adsorption. *RSC Adv.* **2019**, *9* (27), 15642−15647.
(53) Senevirathna, H. L.; Wu, S.; Lee, C.; Kim, J. Y.; Kim, S. S.; Bai, K.; Wu, P. Enhancing MgO Efficiency in CO2 Capture: Engineered MgO/Mg(OH)2 Composites with Cl−, SO42−, and PO43− Additives. *RSC Adv.* **2023**, *13* (40), 27946−27955.
(54) Gutierrez-Ortega, A.; Nomen, R.; Sempere, J.; Parra, J. B.; Montes-Morán, M. A.; Gonzalez-Olmos, R. A Fast Methodology to Rank Adsorbents for CO2 Capture with Temperature Swing Adsorption. *Chem. Eng. J.* **2022**, *435*, 134703.
(55) Zhang, Z.; Huang, W.; Li, X.; Wang, X.; Zheng, Y.; Yan, B.; Wu, C. Water-Stable Composite of HKUST-1 with Its Pyrolysis Products for Enhanced CO2 Capture Capacity. *Inorg. Chem. Commun.* **2022**, *146*, 110063.
(56) Loera-Serna, S.; Cortés-Suárez, J.; Sanchez-Salas, R.; Ramírez-Rosales, D.; Oliver-Tolentino, M.; Ramos-Fernández, E. V. CO2 Adsorption on a Water-Resist HKUST-1 by Incorporation of Graphene Oxide. *Adsorption* **2025**, *31* (1), 5.
(57) Sakai, M.; Ito, A.; Matsumoto, T.; Matsukata, M. One-Pot Synthesis of HKUST-1 Monolith for CO2 Adsorption. *Chem. Lett.* **2024**, *53* (6), upae109.
(58) Shang, S.; Tao, Z.; Yang, C.; Hanif, A.; Li, L.; Tsang, D. C. W.; Gu, Q.; Shang, J. Facile Synthesis of CuBTC and Its Graphene Oxide Composites as Efficient Adsorbents for CO2 Capture. *Chem. Eng. J.* **2020**, *393*, 124666.
(59) Zhao, Y.; Cao, Y.; Zhong, Q. CO2 Capture on Metal-Organic Framework and Graphene Oxide Composite Using a High-Pressure Static Adsorption Apparatus. *J. Clean Energy Technol.* **2014**, *2*, 34−37.
(60) Girimonte, R.; Sofia, D.; Agrippino, S.; Turano, M.; Testa, F. The Process of CO2 Capture and Reduction: Exploring the Efficacy of Metal-Organic Frameworks (MOFs). *Chem. Eng. Trans.* **2024**, *111*, 577−582.
(61) Fateminia, Z.; Chiniforoshan, H.; Ghafarinia, V. Novel Core/Shell Nylon 6,6/La-TMA MOF Electrospun Nanocomposite Membrane and CO_2 Capture Assessments of the Membrane and Pure La-TMA MOF. *ACS Omega* **2023**, *8* (25), 22742−22751.
(62) Sneddon, G.; McGlynn, J. C.; Neumann, M. S.; Aydin, H. M.; Yiu, H. H. P.; Ganin, A. Y. Aminated Poly(Vinyl Chloride) Solid State Adsorbents with Hydrophobic Function for Post-Combustion CO2 Capture. *J. Mater. Chem. A* **2017**, *5* (23), 11864−11872.

https://doi.org/10.1021/acsomega.5c01493
ACS Omega 2025, 10, 30259−30271